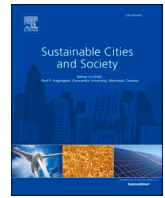




Since January 2020 Elsevier has created a COVID-19 resource centre with free information in English and Mandarin on the novel coronavirus COVID-19. The COVID-19 resource centre is hosted on Elsevier Connect, the company's public news and information website.

Elsevier hereby grants permission to make all its COVID-19-related research that is available on the COVID-19 resource centre - including this research content - immediately available in PubMed Central and other publicly funded repositories, such as the WHO COVID database with rights for unrestricted research re-use and analyses in any form or by any means with acknowledgement of the original source. These permissions are granted for free by Elsevier for as long as the COVID-19 resource centre remains active.



Comparison of COVID-19 infection risks through aerosol transmission in supermarkets and small shops

Chunying Li, Haida Tang^{*}

School of Architecture and Urban Planning, Shenzhen University, Shenzhen 518060, China

ARTICLE INFO

Keywords:

public health
COVID-19
quantitative microbial risk assessment
infection risk
retail building

ABSTRACT

Aerosol transmission is academically recognized as possible transmission route of Coronavirus disease 2019 (COVID-19). We established an approach to assess the airborne-disease infection risks through aerosol transmission based on the dose-response model and aerosol transport model. The accuracy of evaluation was guaranteed with on-site surveyed ventilation rate and occupant behavior. With the proposed approach, COVID-19 infection risks in 5 typical supermarkets and 21 small shops were evaluated. With one original infected early-shift staff, the average aerosols concentrations at steady-state are 1.06×10^{-3} RNA copies/m³ in the supermarkets and 4.73×10^{-2} RNA copies/m³ in the small shops. With the assumption of 5% original infected staff in the retail buildings, the infection probability of one customer is 1.40×10^{-6} for visiting one small shop and 6.22×10^{-6} for visiting one supermarket. The averaged infection risk in the supermarkets is higher than the small shops (p-value < 0.001). On the other hand, the infection risks are higher for the staff working with the infected staff compared with the customers. The proposed approach can be applied to other occupied buildings and assist the pandemic control policy making for sustainable cities and society.

1. Introduction

1.1. Background

Coronavirus disease 2019 (COVID-19) imposed serious damage to the public health and is causing worldwide concern to the person-to-person transmission in buildings (Benita, 2021, Geraldi et al., 2021). Transmission routes of Severe Acute Respiratory Syndrome Coronavirus 2 (SARS-CoV-2) have been widely investigated, covering the large respiratory droplets, airborne aerosol and fomite routes (Desai et al., 2021, Agarwal et al., 2021). With evidence of aerosol transmission confirmed in literature based on reported transmission cases (Morawska & Cao, 2020, Allen & Marr, 2020), the related SARS-CoV-2 aerosol exposure and infection risks are worthy of further study.

Under such circumstance, extensive investigations have been carried out, covering the mechanisms of viral aerosols generation and emission from the respiratory tract during breathing, talking, coughing and sneezing (Mao et al., 2020), particle sizes distribution and viral concentration (Morawska et al., 2009), indoor transport and deposition (Zhou & Ji, 2021), biological decay rate and dose-response analysis (Zhang et al., 2020). Gupta et al. (Gupta et al., 2010) confirmed aerosols

dissipated quickly within 1 m from the mouth. While larger droplets fall to the surrounding surfaces quickly, smaller particles (with diameter less than 10 µm) deposition onto upward, downward and vertical surfaces at different rates. Van Doremalen et al. (Van Doremalen et al., 2020) indicated similar half-lives of SARS-CoV-2 as SARS-CoV-1, which was about 1.1–1.2 h in the environment of 21–23°C temperature and 65% relative humidity.

From the aspect of susceptibles, dose-response model is used to link the infection risk with certain amount of exposure dose (Cheng & Liao, 2013). Exposure dose represents the amount of viral units inhaled over exposure period, whereas infection risk represents prediction of the probability of one susceptible getting infected. The quantitative microbial risk assessment (QMRA) of occupational exposure to SARS-CoV-2 in various types of buildings were carried out (Jones et al., 2021, Ren et al., 2021). It is commonly recognized that ventilation volume and exposure duration are of significant importance to SARS-CoV-2 exposure dose (Kong et al., 2021). Pease (Pease et al., 2021) theoretically calculated the potential aerosol transmission and infectivity of SARS-CoV-2 through central ventilation systems, and confirmed the effectiveness of raising outdoor air supplement as a measure of aerosol transmission control. The filtration of HVAC system was also proved to be significant

^{*} Corresponding author: Haida Tang. School of Architecture and Urban Planning, Shenzhen University, Shenzhen 518060, China. Tel.: 860755-8670-4205.
E-mail address: tanghd@szu.edu.cn (H. Tang).

in lowering the aerosol concentration. Similarly, air flow rate in the South China Seafood Market was considered as important boundary condition in the assessment of COVID-19 infection risk. (Zhang et al., 2020) Though the field survey data (air change rates, customer inlet flow and dwell time) can better guarantee the accuracy of assessment, they were usually unavailable. In the existing literature, assumption values for exposure duration and ventilation volume were commonly applied. Whereas the air flow velocity was calculated through CFD simulation and airflow network analysis in Ref. (Zhang et al., 2020) due to the lack of field-measurement.

1.2. Research objectives

Transmission of airborne disease such as COVID-19 in built environment raises worldwide attention and extensive researches are endowed. The accurate prediction on disease transmission consists of 3 levels: Firstly, the practical ventilation and occupant behavior needs to be collected, whereas few literatures cover these two aspects simultaneously. Secondly, the relationship between the inhaled virus by susceptibles with viral aerosols shedding from the infectors. Thirdly, the infection risk prediction based on the inhaled viral aerosol, i.e., the possibility of one person being infected after inhalation of certain viral aerosols dose.

The present study aims to establish an approach, which gives more accurate evaluation of airborne disease (taking COVID-19 as an example) in occupied spaces and assists to making better pandemic control policy. For each individual, the risk represents the probability of his/her infection. As for the overall occupant, the risk can be transcribed to the predicted infection numbers, which relates closely with the disease transmission on community or city population level. From this perspective, the occupant behavior and air change rate (ACH) within the built environment are on-site surveyed. To acquire the inhaled viral aerosols, the aerosol transport model is applied to assess the viral concentration based on the viral shedding from the infector (or infectors). Dispersion in the air, filtration by air-conditioning system, deposition on surfaces and biologic decay of the virus are taken into consideration. The dose-response model is utilized to evaluate the infection risk from exposed viral dose, i.e., the integral deposition in the human respiratory tract.

The major advancement of the proposed approach is the combination of occupant behavior and air change rate from on-site survey, which better represents the real condition and guarantees the accuracy of the infection risks evaluation. To our knowledge, it is novel to introduce occupant behavior to the prediction of airborne disease transmission in built environment. The evaluation results can better reflect the temporal infection risks on both individual and group level.

1.3. Outline

The proposed approach is applied to evaluate the infection risks of COVID-19 through aerosol transmission route in 26 retail buildings in Shenzhen, China. The paper is organized as following: Part 1 demonstrates the research background and objectives. The research methodology is introduced in Part 2, with calculation results demonstrated in Part 3. Main findings and limitations are discussed in Part 4, with main conclusions presented in Part 5.

2. Method and materials

2.1. General approach

The present study contributes to the existing COVID-19 Quantitative microbial risk assessment (QMRA) with a wholesome approach that covers both internal and external factors. Internal factors refer to the uncontrollable issues influencing aerosol disease transmission, including the viral shedding rate by the infectors, biologic decay of the

virus, as well as the risk of infection with certain amount of viral inhalation. The viral shedding of infectors and dose-response of susceptibles can be gender-, age-, or race-dependent, yet are treated as unanimous in the present stage of investigation. External factors include the controllable (or partly controllable) parameters, including the exposure duration, the viral dilution by ventilation and capture by filtration. The functioning of these factors in the dose-response theory-dominant approach is illustrated in Fig. 1.

2.2. Building information from on-site survey

The proposed infection risk assessment approach is applied to retail buildings in Shenzhen, China. In total 5 supermarkets (within shopping malls) and 21 small shops (diverse in sizes and merchandised goods in residential communities) are surveyed during June and July 2020 (Li et al., 2021). Considering mega-cities such as Shenzhen (with over 20 million population), the confined and crowded retail spaces are likely to impose airborne disease infection risk to the customers and staff.

The dwell time of customers and air change rates are on-site measured, with detailed information available in (Li et al., 2021). Five types of small shops are taken into consideration, including convenient stores, vegetable and meat shops, bakeries, fruit shops, as well as grain, oil and fast food shops. The small shops are all located beside the street where nearby residents purchase daily necessities. The indoor space and volume were measured with laser range finder and calculated for each retail building. For the small shops, the floor areas vary in the range of 21.3~46.8 m², averaged at 33.4 m². As for the supermarkets, the public areas range from 1450.2 to 8456.6 m². The on-site survey was carried out on typical weekdays (throughout the business hours), and the total customer flow was 19436 for the 5 supermarkets and 11124 for the 21 small shops. The average dwell time of customers in the supermarkets (23.5 min) was longer than the combination of 5 types of small shops (17.3 min).

The ventilation rates of the supermarkets and small shops were obtained through consistent measurement of the tracer gas (CO₂ from occupant breathing was used because of safety concern). The CO₂ concentrations of both indoor and outdoor were measured with TelAire (GE7001). Detailed information including the instruments accuracy and measuring points distribution are available in (Li et al., 2021). As the time varying indoor CO₂ was resulted from the change of the occupant number, the variation of the indoor CO₂ can be described as Eq. 1.

$$\frac{dC_{in}}{dt} = ACH(C_{out} - C_{in}) + N \cdot \frac{k}{V} \quad (1)$$

Where C_{in} and C_{out} are the indoor and outdoor CO₂ concentration (ppm). ACH is the outdoor air change rate (h⁻¹). V is the volume of the space (m³). N is the occupants number (-). k is the CO₂ emission rate of each occupant (m³/h), and average value of $k=0.018$ m³/h for male and female customers is used (Li et al., 2014).

Accordingly, the outdoor air change rate can be calculated by the maximum likelihood estimation with the dynamic model of the indoor CO₂ concentration. The obtained ACH reflected the average value of the ACH during the day. According to survey results, the average air change rate was 0.70 h⁻¹ for the supermarkets with mechanical ventilation. As for the small shops, natural ventilation was in dominant with the doors fully open throughout the day with higher average air change rate of 10.94 h⁻¹. With large areas discrepancy, the fresh air volume of supermarkets (averaged at 15771 m³/h) far exceeded that of small shops (784 m³/h). For the 26 retail buildings, the relative uncertainties of ACH was in the range of 12.7 %-15.4 %, with average value of 13.9 %.

2.3. Aerosol transport model

The viral aerosol concentration in enclosed space is dependent on the emission from source, dilution by fresh air, deposition to multiple sur-

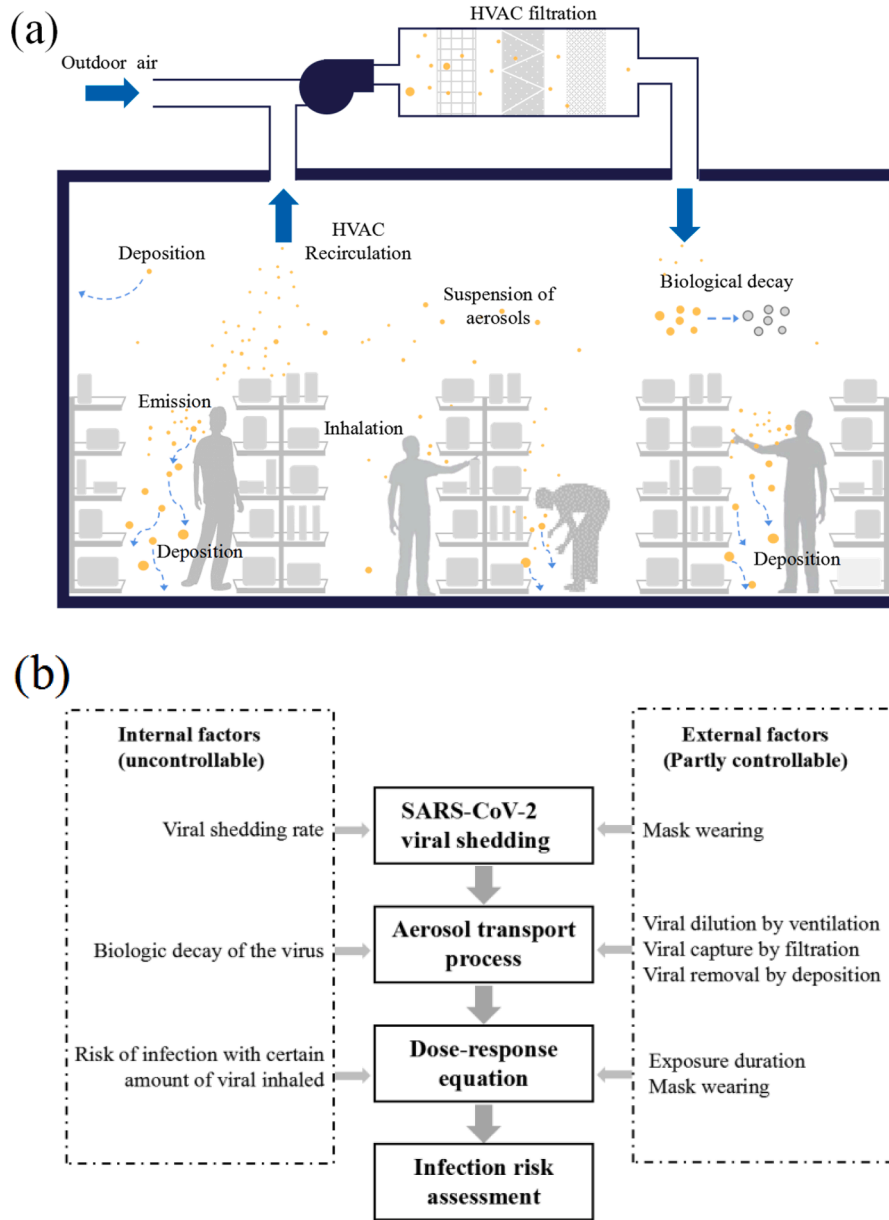


Fig. 1. Infection risk assessment approach: (a) dose-response theory; and (b) steps of infection risk assessment.

faces, biological decay of the virus, as well as the filtration by air-conditioning systems. The transport of aerosols is handled discretely in 4 size bins, i.e., $d_{eq}=0.8 \mu\text{m}$ ($i=1$), $1.8 \mu\text{m}$ ($i=2$), $3.5 \mu\text{m}$ ($i=3$), and $5.5 \mu\text{m}$ ($i=4$), with different deposition and filtration rates (Thatcher et al., 2002). d_{eq} is the midpoint diameter of the aerosol particles in equilibrium state after evaporation, namely the residue diameter. With the assumption of homogeneous virus concentrations, the variation of virus concentration can be expressed as Eqs. 2 and 3 (Zhang et al., 2020).

$$V \frac{dC_i}{dt} = -\phi_i V C_i + \sigma_i \quad (2)$$

$$C_i(0) = 0 \quad (3)$$

Where V is inner volume of an enclosed space (m^3), C_i is the viral concentration (RNA copies/ m^3), t represents time (h), ϕ_i represents the total amount of dilution, deposition, filtration and decay of virus, and is defined as the removal rate (h^{-1}). σ_i is the viral shedding rate by the infector (or infectors) (RNA copies/h). It is predictable that the viral concentration would keep zero if there is no infector in the enclosed

space, and increases with the entering of infector (or infectors). The increment reaches a balancing point when the viral production rate equals to the removal rate. The viral concentration at this balancing point shows the long-term exposure risk and is important for the airborne disease transmission control in any occupied spaces.

Based on the assumption of homogeneous virus concentration within the respiratory fluid, the viral shedding rate can be calculated with Eqs. 4 and 5.

$$\sigma_i = M q_{ex} N_i \frac{1}{6} \pi d_0^3 C_{virus} \quad (4)$$

$$d_0 = \frac{d_{eq}}{0.16} \quad (5)$$

Where M is the number of infectors (-), q_{ex} is the exhalation volume, which is set to be 500 mL per inspiration with 3 seconds intervals (Duan, 2013); N_i represents the particle concentration, i.e., 0.084 cm^{-3} ($d_{eq}=0.8 \mu\text{m}$), 0.009 cm^{-3} ($d_{eq}=1.8 \mu\text{m}$), 0.003 cm^{-3} ($d_{eq}=3.5 \mu\text{m}$) and 0.002 cm^{-3} ($d_{eq}=5.5 \mu\text{m}$) (Morawska et al., 2009). d_0 is the initial

diameter of aerosols (μm), and its relationship with the equilibrium diameter d_{eq} is estimated to be linear (Eq. 5) (Nicas et al., 2005). C_{virus} is the viral load in the respiratory fluid (RNA copies/mL), which is dependent on the virus types and infector characteristics.

The total removal rate of virus is calculated with Eq. 6.

$$\phi_i = ACH + \omega_i + \gamma_i + \lambda \quad (6)$$

Where ACH is the outdoor air change rate (h^{-1}), which represents the viral removal by fresh air dilution and is the same for aerosols of different sizes. ω_i (h^{-1}) represents the viral removal rate in size bin i due to filtration when recirculating through the air-handling unit. The particle diameter-dependent filtration efficiency of the air conditioning systems was obtained from Ref. (Zhang, 2018). The averaged filtration removal rates (h^{-1}) for the supermarkets and small shops are illustrated in Fig. 2(a). γ_i represents the viral removal rate by deposition (h^{-1}), which is related to the area and deposition velocity with respect to the upward-facing, downward-facing and vertical surfaces in the space (Thatcher et al., 2002). The particle diameter-dependent deposition rates in supermarkets and small shops were obtained, as illustrated in Fig. 2(b). λ represents the viral removal rate due to biological decay (h^{-1}), which is the same for aerosols of different sizes. It should be noted that biological decay of SARS-CoV-2 is still not clear and largely dependent on the surrounding environment (Agirman et al., 2020). The total viral removal rates of the supermarkets and small shops are presented in Fig. 2(c). In the small shops, the air change rate (average at 10.94 h^{-1}) dominates the viral removal and functions equally on aerosols with different diameters. This explains the similar viral removal rates (as well as the standard deviations) among different aerosols diameters in small shops.

Based on Eqs. 2–6, the analytical solution of viral concentration is deduced as Eq. 7.

$$C_i(t) = C_{i,s} + [C_i(t_0) - C_{i,s}]e^{-\phi_i(t-t_0)} \quad (7)$$

Where $C_{i,s}$ is the viral concentration at the steady state (RNA copies/ m^3), i.e. when the viral removal rate equals to its production rate, and can be calculated with Eq. 8.

$$C_{i,s} = \frac{\sigma_i}{V\phi_i} \quad (8)$$

2.4. Dose-response model

Dose-response model (Eq. 9) has been widely applied to assess the infection risk involved with viral aerosol inhalation (Sun & Zhai, 2020).

$$p = 1 - e^{-d/k} \quad (9)$$

Where p is the infection probability with certain dose of viral inhalation (-), d represents the inhaled virus dose (RNA copies), which can be calculated with Eq. 10. k is a pathogen dependent parameter (RNA copies). q_{in} is the inhalation volume, which is assumed to be equal with q_{ex} (m^3/h). $t-t_0$ is the dwell time of customers or staff (h).

$$d = \sum_{i=1}^4 \int_{t_0}^t q_{in} C_i(\tau) d\tau \quad (10)$$

As aforementioned, the dwell time of customers in the retail buildings under investigation were on-site surveyed. For the supermarkets, the

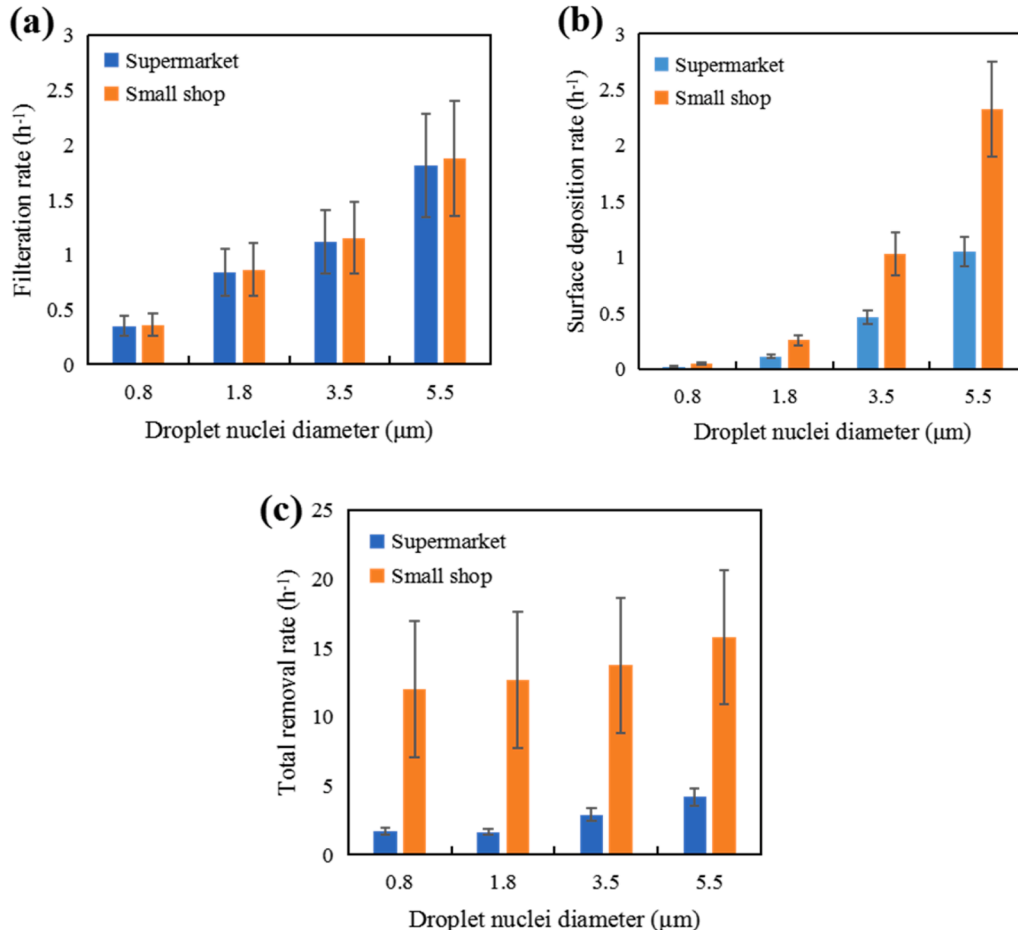


Fig. 2. Removal rate of aerosols: (a) Filtration removal rate; (b) Surface deposition rate; (c) Total removal rate.

customer flow was counted from surveillance videos. The dwell time of each customer in the supermarkets is the time interval between his/her entry and exit time, which were obtained by comparing the surveillance videos at the entry and exit. Approximately 5% customers (i.e., 1373 customers) were selected by interval sampling. Due to lack of surveillance videos in the small shops, we randomly select 10 min per hour to count the customer flow and dwell time. Detailed information is presented in Ref. (Li et al., 2021). Accordingly, the customer flow schedule for each retail building is established: (i) The hourly customer inlet flow numbers are available and the entering time of each customer is confirmed. (ii) The dwell time of each customer is treated as stochastic, which is randomly picked from the dwell time data set (obtained from surveillance videos for the supermarkets and on-site observation for the small shops). (iii) The exit time of each customer is determined with his/her entry time and dwell time.

2.5. Virological properties of SARS-CoV-2

The respiratory droplets are generated by three modes, including the bronchiolar fluid film burst mode, the laryngeal mode, and oral cavity mode. The expelled droplets by an infector come from every part of the respiratory system. With reference to viral load of SARS-CoV-2 in respiratory fluid, researchers measured the virus concentration of the saliva sample, sputum, throat swab, Posterior oropharyngeal saliva and nasopharyngeal swab through Reverse Transcription-Polymerase Chain Reaction (RT-PCR). Table 1 lists the distinctive values of the viral load in respiratory fluid reported in existing literature (Zhu et al., 2020, Iwasaki et al., 2020, To et al., 2020, Yoon et al., 2020, Zheng et al., 2020, Zou et al., 2020, Wölfel et al., 2020, Pan et al., 2020). The viral load in respiratory fluid presents great individual differences. Though viral loads vary between the respiratory specimen from different part of the respiratory system, the viral load of SARS-CoV-2 in respiratory fluid mainly ranged 10^5 – 10^7 RNA copies/mL with an average value of approximately 10^6 RNA copies/mL. In the present study, the viral load of SARS-CoV-2 was assigned following a log-normal distribution, i.e., $\log_{10}(C_{\text{virus}}) \sim N(6,1)$ and utilized by the Monte Carlo simulations for uncertainty analysis (see Table 2).

The decay rate of SARS-CoV-2 in air was evaluated on the basis of half-life of 1.1–1.2 h at 21–23 °C and 65% RH (Van Doremalen et al.,

Table 1
Viral loads of SARS-CoV-2 in respiratory fluids reported in literature.

Sample sources	C_{virus}
Saliva	(1) 10^4 – 10^8 RNA copies/mL (Zhu et al. (Zhu et al., 2020)) (2) $4.1 \pm 1.4 \log_{10}$ RNA copies/mL (Iwasaki et al. (Iwasaki et al., 2020)) (3) Saliva specimen: median 3.3×10^6 RNA copies/mL (range, 9.9×10^2 to 1.2×10^8 RNA copies/mL) (To et al. (To et al., 2020)) (4) patient 1 = $6.63 \log_{10}$ RNA copies/mL; patient 2 = $7.10 \log_{10}$ RNA copies/mL (Jin et al. (Yoon et al., 2020)) (5) 3.6 – $6.5 \log_{10}$ RNA copies/mL, median $5 \log_{10}$ RNA copies/mL (Zheng et al. (Zheng et al., 2020))
Sputum	(1) 10^3 – 10^4 RNA copies/mL (Zou et al. (Zou et al., 2020)) (2) Average 7×10^6 RNA copies/mL (Wölfel et al. (Wölfel et al., 2020))
Throat	(1) 10^4 – 10^7 RNA copies/mL, median 7.99×10^4 RNA copies/mL (Pan et al. (Pan et al., 2020)) (2) 103 – 104 RNA copies/mL (Zou et al. (Zou et al., 2020))
Posterior oropharyngeal saliva	(1) Severe disease: $6.17 \log_{10}$ RNA copies/mL (IQR 4.18–7.18); Mild disease: $5.11 \log_{10}$ RNA copies/mL (IQR 3.91–7.56) (To et al. (To et al., 2020))
Nasopharyngeal swab	(1) $5.4 \pm 2.4 \log_{10}$ RNA copies/mL (Iwasaki et al. (Iwasaki et al., 2020)) (2) patient 1 = $8.41 \log_{10}$ RNA copies/mL; patient 2 = $7.49 \log_{10}$ RNA copies/mL (Jin et al. (Yoon et al., 2020)) (3) 10^4 – 10^7 RNA copies/mL (Wölfel et al. (Wölfel et al., 2020))

Table 2
Distributions of the virological properties of SARS-CoV-2

Parameter	C_{virus}	λ	k
Unit	RNA copies/mL	h^{-1}	RNA copies
Description	Virus concentration in respiratory fluid	Biologic decay rate of the virus	Pathogen dependent parameter
Distribution	Lognormal distribution	Lognormal distribution	Uniform distribution
Assumed PDF	$\log_{10}(C) \sim N(6,1)$	$\text{LN}(0.63, 0.5)$	$U(10, 100)$
References	(Zhu et al., 2020, Yoon et al., 2020, Wölfel et al., 2020)	(Zhang et al., 2020, Van Doremalen et al., 2020)	(Watanabe et al., 2010)

2020), thus λ was approximately 0.63 h^{-1} . According to the reported biological decay of other corona virus, the measured biological decay of Middle East Respiratory Syndrome (MERS-CoV) in the air ranged 0.5–2.0 h (Pyankov et al., 2018) and that of the common Human Coronavirus (HCoV) ranged 3.3–100 h (Ijaz et al., 1985). The half-life periods of corona virus ranged 0.5–100 h. Therefore, the biological decay of SARS-CoV-2 in the air was assigned following a log-normal distribution, i.e., $\lambda \sim \text{LN}(0.63, 0.5)$ for uncertainty analysis (see Table 2). To our best knowledge, there are currently no values available in literature for the pathogen dependent parameter related to the infectivity (k) for SARS-CoV-2. Under such circumstance, the value of k was determined with reference to Ref. (Watanabe et al., 2010), in which the SARS-CoV infectious dose was 10–100 RNA copies based on the data for the infection of transgenic mice susceptible to SARS-CoV. In view of the similarity between the SARS-CoV-2 and the SARS-CoV, we adopted the uniform distribution $k \sim U(10, 100)$ with a mean value of 55 RNA copies in order to fully consider the uncertainties. Table 2 lists the distributions of virological properties of SARS-CoV-2 used in this study. We utilized Monte Carlo method for the uncertainty analysis, which is frequently utilized in risk assessment with parameter uncertainties (Zhang et al., 2020). Furthermore, the contributions of the uncertain parameters to the final uncertainty of the infection risk assessment were analyzed with Sobol's method. The main advantages of Sobol's method are the robustness for non-linear models and the comprehensive reflection of influence by each parameter on full variation range (Das et al., 2014).

In the present study, the quantitative microbial risk assessment of SARS-CoV-2 was conducted with the assumption of only one infected staff in every retail building. The retailers run in two-shift operation with business hours from 8 am to 10 pm. Two scenarios are considered in the calculation: (i) an early-shift staff (on duty from 7 am to 3 pm) is COVID-19 infector; (ii) a night-shift staff (on duty from 3 pm to 11 pm) is COVID-19 infector. The infected staff is assumed to be asymptomatic. Here, asymptomatic infector refers to people who are infected but never develop symptoms during the period of infection and throughout working hours, thus no exceptional events (such as coughing and sneezing) are considered.

3. Results

3.1. Viral concentration in retailing buildings

The temporal viral aerosol concentrations in the retail buildings were calculated with aerosol transport model. Fig. 3 shows the variation of viral concentrations in the 1st supermarket, with the colored curves representing different aerosol sizes. The viral load of SARS-CoV-2 in respiratory fluid was set as 10^6 RNA copies/mL. The biological decay of SARS-CoV-2 in the air was set as 0.63 h^{-1} .

As illustrated in Fig. 3(a), the viral aerosol concentrations in the supermarket increase since 7am, with the arriving of the infected early-shift staff. The concentrations reach a stable point at around 8am for larger aerosols ($d_{eq}=5.5 \mu\text{m}$), and at 9–10am for the smaller particles.

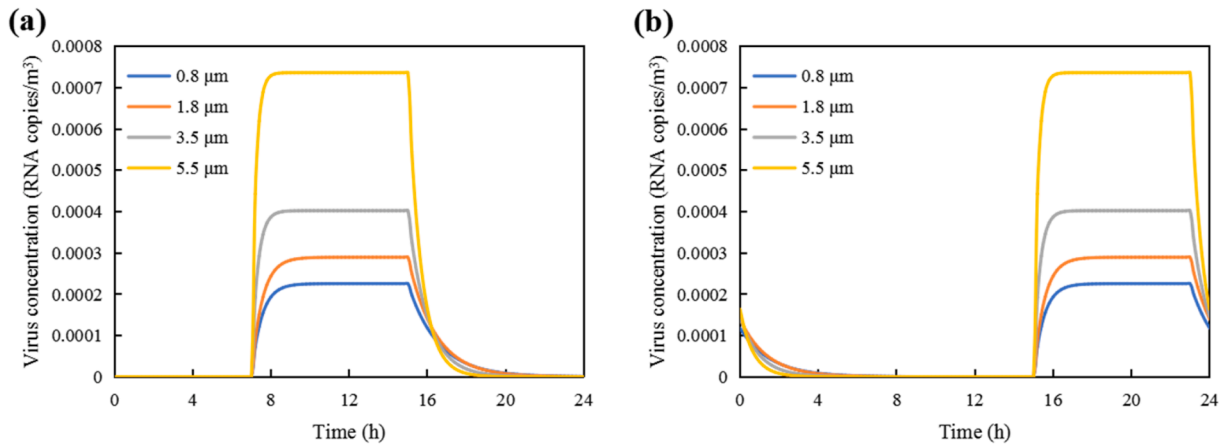


Fig. 3. Variation of viral aerosol concentrations in the 1st supermarket: (a) the infected staff is on early shift; and (b) the infected staff is on late shift.

The stable state represents the equilibrium of emission rate and removal rate. Before this stable state, the viral aerosols increase as the removal viral aerosols is less than the aerosols emitted. In other words, the viral concentration (C_i) is so small that the right part of Eq. 1 is positive, which means the left part of Eq. 1 is also positive and C_i keeps increasing. As the removal rate (ϕ_i) of larger aerosols is bigger than small ones (see Fig. 2(c)), the right part of Eq. 1 decreases to zero in a shorter time, i.e., the larger aerosols reach the stable point earlier than the smaller ones. Afterwards, the concentrations remained stable as the aerosols production and removal are balanced. The stable-state virus concentrations were respectively 2.26×10^{-4} , 2.89×10^{-4} , 4.02×10^{-4} and 7.36×10^{-4} RNA copies/ m^3 . Since 3pm, the concentrations of aerosols drop dramatically, as the infected staff left the supermarket. It takes about 5 hours for the viral aerosols being removed through dilution, filtration and deposition. The shapes of the curves in Fig. 3(b) are quite similar as Fig. 3(a), with the rise and drop of viral aerosol concentrations postponed by 8 hours.

The variations of viral aerosol concentrations in the 1st small shop are presented in Fig. 4. The shape of the curves is similar with that of Fig. 3, with sharper increase and drop. The steady-state virus concentrations are 8.25×10^{-2} RNA copies/ m^3 (the sum of viral within aerosols of different sizes) in the 1st small shop.

As illustrated in Fig. 3 and 4, the virus concentrations remain at the steady-state level for most of the time with the infected staff on duty. Therefore, the steady-state concentration is a suitable index representing the viral exposure risk in the confined spaces. The comprehensive virus concentrations (combining the virus within aerosols of different sizes) for each retail buildings are presented in Fig. 5. The average virus concentration is 4.73×10^{-2} RNA copies/ m^3 in the small shops and

1.06×10^{-3} RNA copies/ m^3 in the supermarkets.

3.2. Inhaled virus by customers and staff

The inhaled virus by the occupants is dependent on 3 factors: inspiration rate, virus concentration and dwell time. The inspiration rates of the staff and customers are $0.6 m^3/h$. The viral load of SARS-CoV-2 in respiratory fluid was set as 10^6 RNA copies/mL, with biological decay of $0.63 h^{-1}$. Fig. 6 and Fig. 7 illustrate the inhaled virus by the susceptible customers and staff with one early-shift staff being infected.

In Fig. 6, the inhaled virus by the susceptible early-shift staff is much larger than the late-shift staff. As the SARS-CoV-2 viral concentration of both supermarkets and small shops drop dramatically after the infected staff left (as illustrated in Fig. 3 and 4), the viral concentration is far lower during the working hours of the late-shift staff. The average inhaled virus by an early-shift staff in the 5 supermarkets is 5.80×10^{-3} RNA copies, and 7.16×10^{-4} RNA copies for a late-shift staff. Meanwhile, the amounts of inhaled virus by staff in the small shops (Fig. 6(b)) are larger. The average inhaled virus by early-shift staff in the 21 small shops is 0.22 RNA copies. The dominant influence of steady-state viral concentrations on the total inhalation is obvious from the similar shape of histograms in Fig. 5 and 6.

The customers dwell time in the retail buildings are diversified, and are much shorter than the staff. As a result, the virus inhalation of the customers is far less than the staff and diversely distributed in a wide range, as illustrated in the box-plot of Fig. 7. Each box represents the inhaled virus by the customers in one supermarket or small shop, with the bottom and top edges indicating the 25th and 75th percentiles. The horizontal lines within the box represent the median value. The whiskers

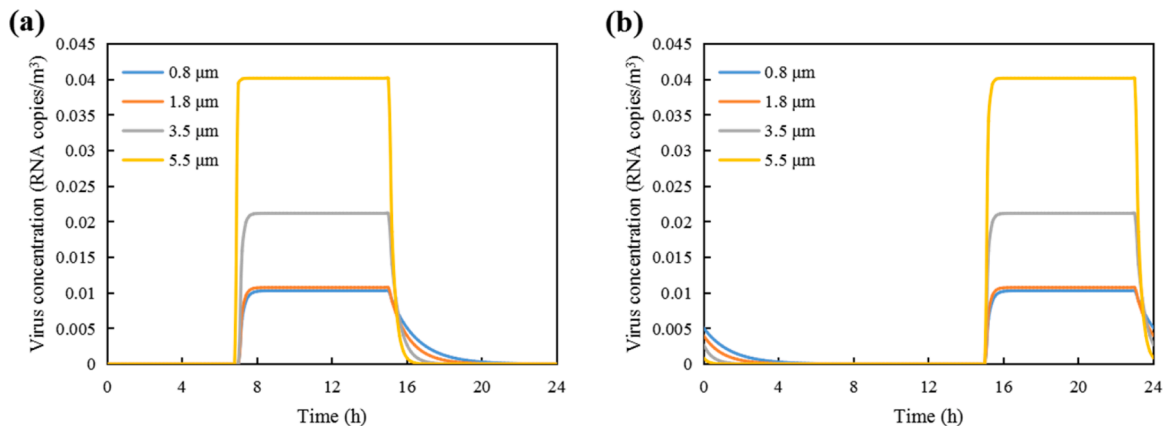


Fig. 4. Variation of viral aerosol concentration in 1st small shop: (a) infected staff is on early shift; and (b) infected staff is on late shift.

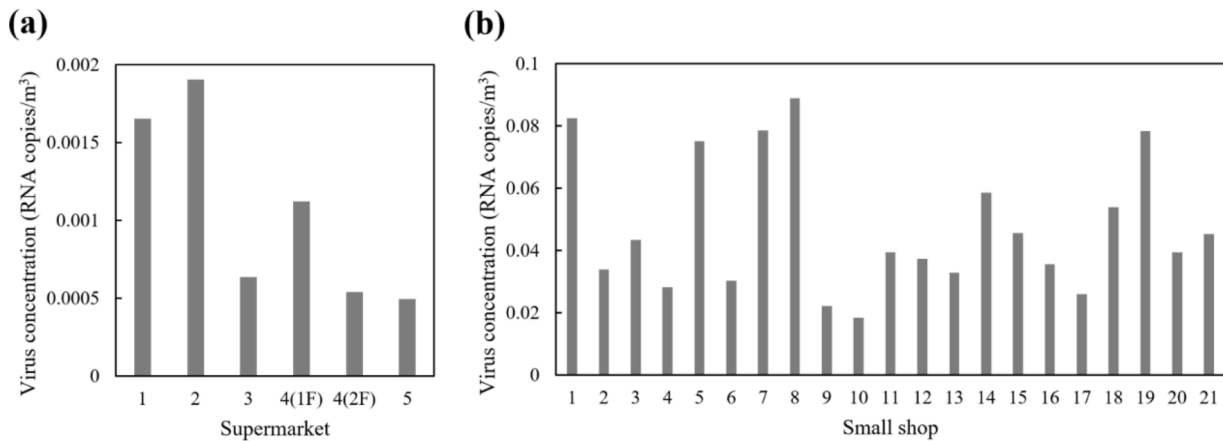


Fig. 5. Steady-state virus concentrations in the retail buildings: (a) supermarkets; and (b) small shops.

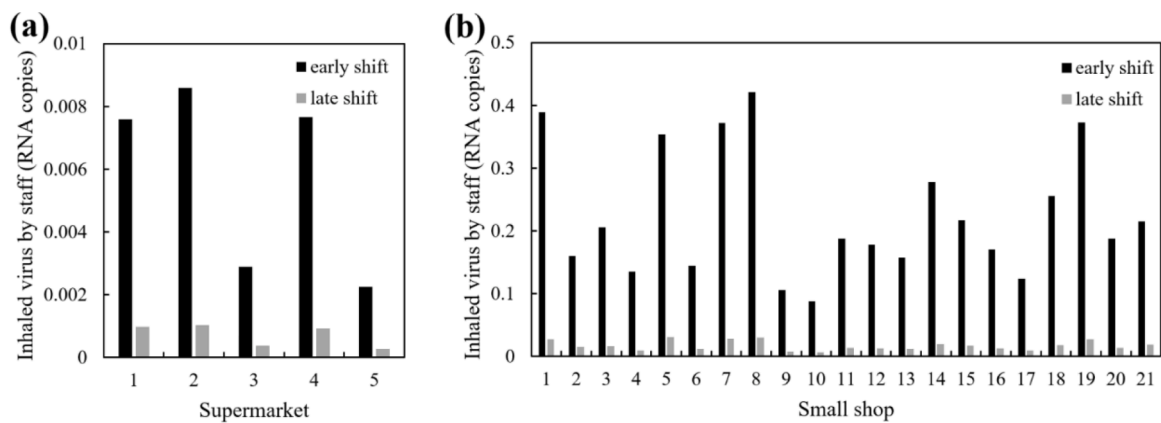


Fig. 6. Inhaled virus dose by the staff: (a) supermarket; and (b) small shops.

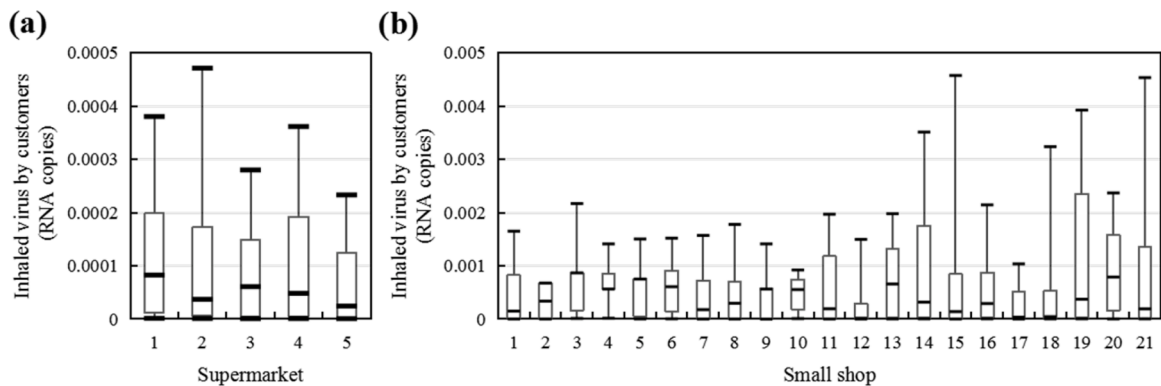


Fig. 7. Inhaled virus by the customers: (a) supermarket; and (b) small shops.

extend to the 5th and 95th percentiles.

In general, the inhaled virus is larger for customers in the small shops. The average median value of virus inhalation is 3.77×10^{-4} RNA copies in small shops, and 5.07×10^{-5} RNA copies in the supermarkets. The worst conditions occur in the 1st supermarket and the 3rd small shop.

3.3. Infection risks through aerosol transmission

As described in Part 2.5, the Monte Carlo method is applied. The distribution and input values of the uncertainties are listed in Table 2. For each retail building, the infection probabilities of customers, early-shift staff and late-shift staff are calculated through 4000 model runs,

with the assumption of one infected staff on early-shift. The distribution patterns of the mean infection probabilities (5th percentiles, average value and 95th percentiles out of 4000 set of results) are depicted in Fig. 8.

The median values of the mean infection probability (the circles in Fig. 8) show the general infection risk levels in each supermarket and small shop. In general, the mean infection probability is the highest for early-shift staff, follows by the late-shift staff and the customers under the condition of one infected early-shift staff. The infection risks are higher in small shops compared with supermarkets. As presented in Fig. 8(b), the median infection probabilities fall in the range of 4.38×10^{-5} – 1.67×10^{-4} among the 5 supermarkets for the early-shift staff, and

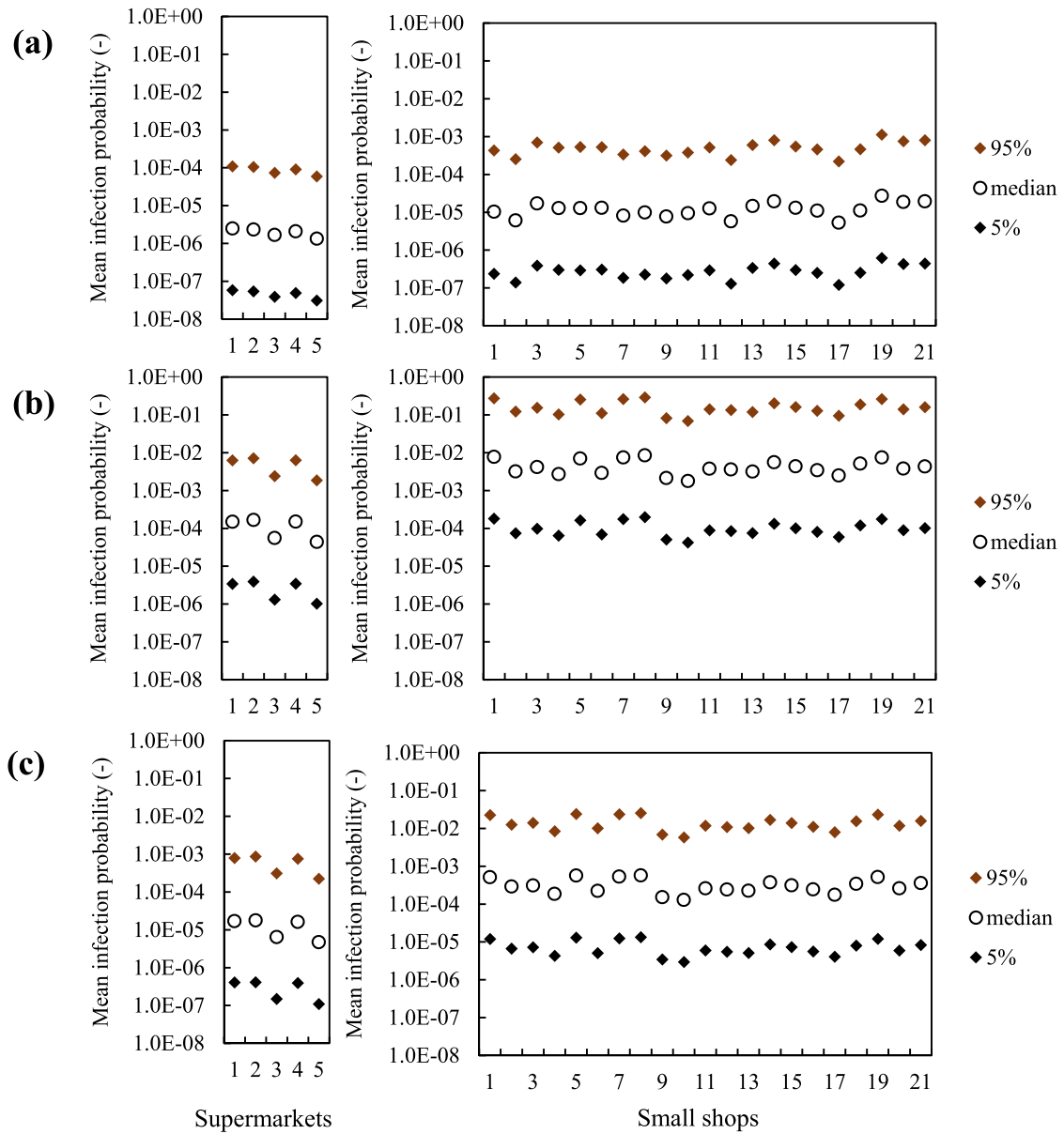


Fig. 8. Infection probability of the susceptibles with one infected early-shift staff: (a) customers; (b) early-shift staff; and (c) late-shift staff.

1.78×10^{-3} – 8.48×10^{-3} among the 21 small shops. As for the late-shift staff (Fig. 8(a)) and the customers (Fig. 8(c)), the median probabilities are much lower in both supermarkets and small shops with distribution ranges narrowed, which reveals relatively lower infection risks.

For the customers (in Fig. 8(a)), the risks drop to 1.33×10^{-6} – 2.49×10^{-6} and 5.33×10^{-6} – 2.73×10^{-5} in supermarkets and small shops. The infection probabilities are similar in different types of small shops. The median values of the mean infection probability of the customers are respectively 1.14×10^{-5} , 1.17×10^{-5} , 9.86×10^{-6} , 1.93×10^{-5} and 1.91×10^{-5} , for the convenience store, vegetable and meat shop, bakery, fruit shop and the grain, oil & fast food shop. Meanwhile, the infection probability of the late-shift staff in the small shops is over one order of magnitude higher than that of the customers. This is due to the great difference of dwell time, with 8h working hours of the staff and 0.06h average dwell time of customers. It is noticeable that 95th percentile value of the mean infection probability is approximately 3 orders of magnitude higher than the 5th percentile value. It shows that the value ranges of the virological properties of SARS-CoV-2 play an important role in the infection risks.

3.4. Sensitivity analysis

Sensitivity analysis of the virological properties of SARS-CoV-2 on the infection risk assessment is carried out with Sobol's method. The one-order sensitivity index and total sensitivity index of C_{virus} , λ and k are depicted in Fig. 9.

Fig. 9 shows the dominant influence of the viral load in respiratory fluid (C_{virus}) on the infection risk assessment, following with the dose-response related parameter (k) and biological decay rate (λ). It is commonly acknowledged that C_{virus} is largely dependent on individual characteristics of the infector and the stage in the course of disease, as well as the respiratory fluid sources (see Table 1). This results in a wide-range distribution of C_{virus} , and explains the higher sensitivity index of C_{virus} in Fig. 9.

Comparatively, the sensitivity index of λ is much lower. In the present study, the bio-decay related viral removal rate is much less compared with the filtration and surface deposition-related viral removal rate (See Fig. 2). In other words, the distribution of C_{virus} can alter the indoor viral concentration with up to 100 folds. Considering that the viral removal through biological decay accounts for 39.5 % of

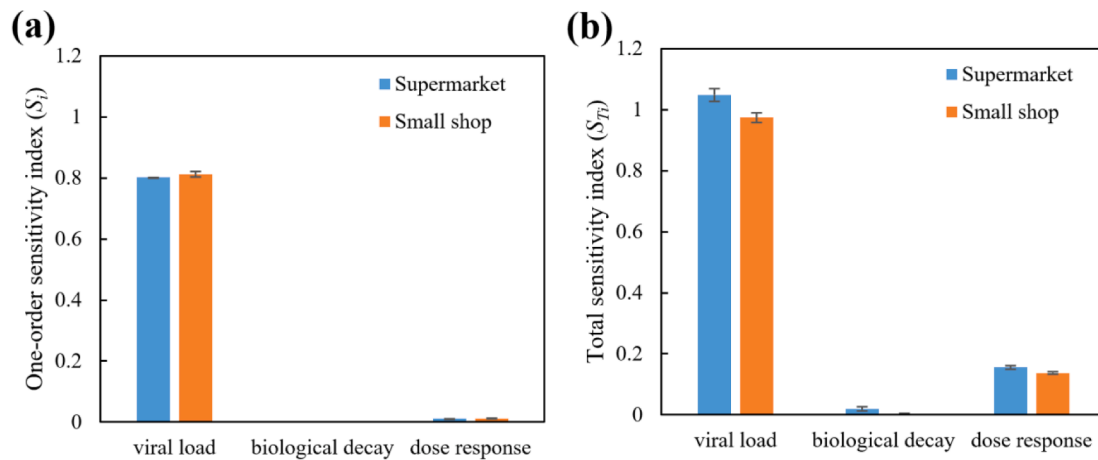


Fig. 9. Sensitivity analysis results with Sobol's method: (a) one-order sensitivity index; and (b) total sensitivity index.

the total removal rate, the influence of λ on indoor viral concentration is much less significant compared with C_{virus} . In summary, the sensitivity analysis results indicate the significance of further investigation on the dose-response of SARS-CoV-2, so that infection risk prediction can be more accurate.

4. Discussions

4.1. Infection risks in retail buildings

The present study evaluates the airborne disease infection risks of staff and customers in typical supermarkets and small shops. The on-site survey provides first-hand data concerning the customer flow and ventilation rate. In Part 3.2 and 3.3, the inhaled viral dose and infection risk of purchasing in different retail buildings are compared, based on the assumption of one infected staff in every supermarket and small shop. Considering that the staff number in the supermarkets (averaged at 63.1) are much more than the small shops (averaged at 2.2), the probability of staff being infected is much higher for supermarkets. Therefore, the results are expanded to better compare the infection risks in supermarkets and small shops. Here, the 5% probability of original infected staff was applied. As a result, the infection probability of the customer is 1.40×10^{-6} (average value) for visiting one small shop and 6.22×10^{-6} (average value) for visiting one supermarket. The averaged infection risk in the supermarkets is higher than the small shops (p -value < 0.001). According to the field survey, the purchasing in five different small shops (including convenient stores, vegetable and meat shops, bakeries, fruit shops, grain, oil and fast food shops) can be marginally equivalent to one supermarket. With this assumption, the infection probability of one customer is 7.87×10^{-6} after visiting five different small shops to purchase daily necessities, which is 26.6 % higher than that of a supermarket with an identical original infected staff proportion of 5%.

Based on the calculation results, airborne transmission control measures are suggested for retail buildings. First of all, mechanical ventilation should supply sufficient fresh air to dilute the viral aerosols. Occupant-density-detection based energy efficient ventilation system can be adopted to dilute the viral aerosols with preferable energy efficiency. (Wang et al., 2021) High filtration efficiency is desirable to remove the viral aerosols from recirculated air. Secondly, movable filtration equipment with UV can be utilized to assist the aerosol removal, which should be placed in crowded locations. (Feng et al., 2021) Thirdly, the infection risks can be reduced by shortening the customers dwell time. Strategy of intermittent occupancy can be adopted in small shops to reduce the airborne transmission risks. (Melikov et al., 2020) Last but not least, it is important for all staff and customers

to wear face masks during working/shopping. The function of face masks wearing in preventing COVID-19 has been thoroughly summarized in (Liao et al., 2021).

In (Zhang et al., 2020), the COVID-19 infection risk through aerosol transmission in a natural ventilated seafood market was calculated to be 2.23×10^{-5} (median value) after 1h exposure with one infected staff in the market. This is higher than the median infection probabilities (1.33×10^{-6} – 2.49×10^{-6}) during one visit of supermarket (with one infected staff) in our study. The main reasons are: (i) The larger ventilation rate in the supermarkets under survey is the straightforward factor accounting for the low virus concentration and infection risks. In (Zhang et al., 2020), the CFD simulation results revealed 0.35 m/s average airflow velocity within the 70 m length walking aisle. Accordingly, the air change rate was 0.18 h^{-1} , which is far less than the supermarkets (0.72 h^{-1}) in our study. (ii) The average dwell time of the supermarkets is 23.5min, which is 39.2% of the dwell time in the seafood market.

In (Dada & Gyawali, 2021), the individual infection risk of working staff in waste-water treatment plants is evaluated to be 0.036 per 1000 exposed WWTP operators with low grade outbreak scenarios (similar as the present study). The corresponding risk per exposure is 3.6×10^{-5} . This risk is comparable with the median infection probabilities of early-shift staff in supermarkets (4.38×10^{-5} – 1.67×10^{-4} , co-work with one infected staff). Meanwhile, a higher infection risk of 0.19–1.88% in out-patient waiting rooms was evaluated in (Li & Tang, 2021). The higher risk was mainly caused by the setting of 2% infected occupants within the enclosed spaces with high occupant density. That setting corresponds to a develop stage of pandemic, instead of the early stage assumption in the present study.

In general, the proposed approach offers a decision-making tool to assess the airborne disease infection risk in public buildings. The approach is both practical (real data can be obtained with on-site survey at low cost) and robust (parameter uncertainties were taken into consideration). It can be included to forecasting models, providing the risks of general population during shopping, working, studying and leisure activities. (Ribeiro et al., 2020) To a larger extent, the pandemic development on the community or city scale can be summarized and induced based on the present approach and related population mobility big data. Artificial intelligence, climate data and built environment can be involved in the evaluation, as discussed in (da Silva et al., 2020, Mouratidis, 2021, Liu et al., 2021). The results can guide the policy makers fully understand and prepare for the situation, as well as to improve the built environment. (Megahed & Ghoneim, 2020, Guo et al., 2021)

4.2. Limitations

The present study provides good assist for infection risk control and related policy making. The following limitations should be noted: (i) Only aerosol transmission of COVID-19 is assessed. Though the social distancing policy is commonly adopted in public buildings, the transmission routes of large respiratory droplets and fomite contact cannot be excluded in shopping scenario. (ii) The viral concentration of SARS-CoV-2 in the retail buildings are treated as homogeneous. This assumption is based on following reasons: First of all, the infected staff keeps moving in the supermarkets and small shops and emitting viral aerosol at different locations of the space. Afterwards, the emitted viral aerosols are dispersed with the walking and moving of the working staff and customers. Lastly, the air-conditioning system keeps on operation during business hour, and the viral aerosols are further blended at the air-handling unit with return air before supplied to the diffusers. (iii) The uncertainty parameters (such as the deposition rate of the aerosol particles and the evaporation rate of the exhaled aerosols) brought errors into the calculated infection risks. (iv) The personal protection measures (such as surgical mask wearing) are not included.

Due to the limited time and labor, the on-site survey was carried out only in summer. It should be noted that the air change rate of the same retail building is likely to be different in each season. In the future, this approach can be applied in other sorts of occupied buildings with the assist of CO₂ online monitoring system (to calculate the air change rate) and artificial intelligence (to detect occupant behavior). Additionally, the future study should cover the transmission routes of large respiratory droplets and fomite contact, as well as utilizing more CO₂ concentration monitoring devices in larger space to better understand the distribution of indoor air freshness. Meanwhile, the personal protection measures, such as mask wearing, should be taken into account by adjusting the virus shedding rate and the dose-inhalation value for the development stage of pandemic in future studies.

5. Conclusions

Accurate evaluation of airborne-disease infection risk in buildings is important for pandemic control and sustainable cities and society. The present study establishes a novel approach for the evaluation of infection risks through aerosol transmission. The innovative approach bases on the dose-response model and aerosol transport model, and combines occupant behavior and air change rate from on-site survey, which better reflects the real condition and guarantees the accuracy of evaluation. The SARS-CoV-2 viral aerosols concentrations and consequent infection risks with the assumption of one asymptomatic infected staff in the confined space were calculated for 5 supermarkets and 21 small shops in Shenzhen, China. The main findings are as following:

- (1) With the assumption of one infected early-shift staff, the steady-state virus concentrations of the small shops (4.73×10^{-2} RNA copies/m³) are higher than the supermarkets (1.06×10^{-3} RNA copies/m³).
- (2) With the assumption of 5% original infected staff in the retail buildings, the infection probability of one customer is 1.40×10^{-6} for visiting one small shop and 6.22×10^{-6} for visiting one supermarket.
- (3) Considering the customers purchasing demand, visiting five different small shops for daily necessities can be marginally equivalent to one visit to a supermarket. The infection probability of one customer is 7.87×10^{-6} after visiting five different small shops to purchase daily necessities, which is 26.6% higher than that of one supermarket.
- (4) The COVID-19 infection risks of the staff are higher than the customers. Possible measures to reduce the risks include higher level of air change rate and filtration efficiency with mechanical ventilation, as well as surgical mask wearing.

- (5) The proposed approach can be applied to other buildings where occupants share enclosed spaces. With its assistance, places with high infection risks can be spotted, and pandemic control measures can be more goal-oriented and efficient.

Declaration of Competing Interest

We declare that we have no financial and personal relationships with other people or organizations that can inappropriately influence our work, there is no professional or other personal interest of any nature or kind in any product, service and/or company that could be construed as influencing the position presented in, or the review of, the manuscript entitled "Comparison of COVID-19 infection risks through aerosol transmission in supermarkets and small shops".

Acknowledgments

The study described in this paper was supported by the National Natural Science Foundation of China (No. 52078296, No. 51808343, and No. 52008254).

References

- Benita, F. (2021). Human mobility behavior in COVID-19: A systematic literature review and bibliometric analysis. *Sustainable Cities and Society*, 70, Article 102916.
- Geraldi, M. S., Bavaresco, M. V., Triana, M. A., Melo, A. P., & Lamberts, R. (2021). Addressing the impact of COVID-19 lockdown on energy use in municipal buildings: A case study in Florianópolis, Brazil. *Sustainable Cities and Society*, 69, Article 102823.
- Desai, P. S., Sawant, N., & Keene, A. (2021). On COVID-19-safety ranking of seats in intercontinental commercial aircrafts: A preliminary multiphysics computational perspective. *Build. Simul.*, 14, 1585–1596.
- Agarwal, N., Meena, C. S., Raj, B. P., Saini, L., Kumar, A., Gopalakrishnan, N., Kumar, A., Balam, N. B., Alam, T., Kapoor, N. R., & Aggarwal, V. (2021). Indoor air quality improvement in COVID-19 pandemic. *Sustainable Cities and Society*, 70, Article 102942.
- Morawska, L., & Cao, J. (2020). Airborne transmission of SARS-CoV-2: The world should face the reality. *Environment international*, 139, Article 105730.
- Allen, J. G., & Marr, L. C. (2020). Recognizing and controlling airborne transmission of SARS-CoV-2 in indoor environments. *Indoor air*, 30(4), 557.
- Mao, N., An, C. K., Guo, L. Y., Wang, M., Guo, L., Guo, S. R., & Long, E. S. (2020). Transmission risk of infectious droplets in physical spreading process at different times: a review. *Building and Environment*, Article 107307.
- Morawska, L., Johnson, G. R., Ristovski, Z. D., Hargreaves, M., Mengersen, K., Corbett, S., Chao, C. Y. H., Li, Y., & Katoshevski, D. (2009). Size distribution and sites of origin of droplets expelled from the human respiratory tract during expiratory activities. *Journal of aerosol science*, 40(3), 256–269.
- Zhou, Y., & Ji, S. (2021). Experimental and numerical study on the transport of droplet aerosols generated by occupants in a fever clinic. *Building and Environment*, 187, Article 107402.
- Zhang, X., Ji, Z., Yue, Y., Liu, H., & Wang, J. (2020). Infection risk assessment of COVID-19 through aerosol transmission: a case study of South China Seafood Market. *Environmental science & technology*, 55(7), 4123–4133.
- Gupta, J. K., Lin, C. H., & Chen, Q. (2010). Characterizing exhaled airflow from breathing and talking. *Indoor air*, 20(1), 31–39.
- Van Doremalen, N., Bushmaker, T., Morris, D. H., Holbrook, M. G., Gamble, A., Williamson, B. N., Azaibi, T., Jennifer, L., Harcourt, Natalie, J. Thornburg, Susan, I., Gerber, James, O., Lloyd-Smith, Emmie De Wit, & Munster, V. J. (2020). Aerosol and surface stability of SARS-CoV-2 as compared with SARS-CoV-1. *New England journal of medicine*, 382(16), 1564–1567.
- Cheng, Y. H., & Liao, C. M. (2013). Modeling control measure effects to reduce indoor transmission of pandemic H1N1 2009 virus. *Building and environment*, 63, 11–19.
- Jones, B., Sharpe, P., Iddon, C., Hathway, E. A., Noakes, C. J., & Fitzgerald, S. (2021). Modelling uncertainty in the relative risk of exposure to the SARS-CoV-2 virus by airborne aerosol transmission in well mixed indoor air. *Building and environment*, 191, Article 107617.
- Ren, C., Xi, C., Wang, J., Feng, Z., Nasiri, F., Cao, S. J., & Haghighat, F. (2021). Mitigating COVID-19 Infection Disease Transmission in Indoor Environment Using Physical Barriers. *Sustainable cities and society*, Article 103175.
- Kong, X., Guo, C., Lin, Z., Duan, S., He, J., Ren, Y., & Ren, J. (2021). Experimental study on the control effect of different ventilation systems on fine particles in a simulated hospital ward. *Sustainable Cities and Society*, Article 103102.
- Pease, L. F., Wang, N., Salisbury, T. L., Underhill, R. M., Flaherty, J. E., Vlachokostas, A., Kulkarni, G., & James, D. P. (2021). Investigation of potential aerosol transmission and infectivity of SARS-CoV-2 through central ventilation systems. *Building and Environment*, 197, Article 107633.
- Li, C., Tang, H., Wang, J., Zhong, Z., Li, J., & Wang, H. (2021). Field study to characterize customer flow and ventilation rates in retail buildings in Shenzhen, China. *Building and Environment*, 197, Article 107837.

- Li, H., Li, X., & Qi, M. (2014). Field testing of natural ventilation in college student dormitories (Beijing, China). *Building and environment*, 78, 36–43.
- Duan, X. (2013). *Exposure factors handbook of Chinese population*[M]. Beijing, China: China Environmental Science Press.
- Morawska, L. J. G. R., Johnson, G. R., Ristovski, Z. D., Hargreaves, M., Mengersen, K., Corbett, S., Chao, C. Y. H., Li, Y., & Katosheviski, D. (2009). Size distribution and sites of origin of droplets expelled from the human respiratory tract during expiratory activities. *Journal of aerosol science*, 40(3), 256–269.
- Nicas, M., Nazaroff, W. W., & Hubbard, A. (2005). Toward understanding the risk of secondary airborne infection: emission of respirable pathogens. *Journal of occupational and environmental hygiene*, 2(3), 143–154.
- Zhang, H. L. (2018). Experimental Study of Filters of Different Grades on Outdoor Airborne Particulate Matter. *Xi'an, Xi'an University of Architecture and Technology* (in Chinese).
- Thatcher, T. L., Lai, A. C., Moreno-Jackson, R., Sextro, R. G., & Nazaroff, W. W. (2002). Effects of room furnishings and air speed on particle deposition rates indoors. *Atmospheric environment*, 36(11), 1811–1819.
- Agirman, A., Cetin, Y. E., Avci, M., & Aydin, O. (2020). Effect of air exhaust location on surgical site particle distribution in an operating room. *Build. Simul.*, 13, 979–988.
- Sun, C., & Zhai, Z. (2020). The efficacy of social distance and ventilation effectiveness in preventing COVID-19 transmission. *Sustainable cities and society*, 62, Article 102390.
- Zhu, J., Guo, J., Xu, Y., & Chen, X. (2020). Viral dynamics of SARS-CoV-2 in saliva from infected patients. *Journal of Infection*, 81(3), 48–50.
- Iwasaki, S., Fujisawa, S., Nakakubo, S., et al. (2020). Comparison of SARS-CoV-2 detection in nasopharyngeal swab and saliva. *Journal of Infection*, 81(2), 145–147.
- To, K. K. W., Tsang, O. T. Y., Yip, C. C. Y., et al. (2020). Consistent detection of 2019 novel coronavirus in saliva. *Clinical Infectious Diseases*, 71(15), 841–843.
- Yoon, J. G., Yoon, J., Song, J. Y., et al. (2020). Clinical significance of a high SARS-CoV-2 viral load in the saliva. *Journal of Korean medical science*, 35(20), 195.
- Zheng, S., Fan, J., & Yu, F. (2020). Viral load dynamics and disease severity in patients infected with SARS-CoV-2 in Zhejiang province, China, January–March 2020: retrospective cohort study. *bmj*, 369.
- Zou, L., Ruan, F., Huang, M., et al. (2020). SARS-CoV-2 viral load in upper respiratory specimens of infected patients. *New England Journal of Medicine*, 382(12), 1177–1179.
- Wölfel, R., Corman, V. M., Guggemos, W., et al. (2020). Virological assessment of hospitalized patients with COVID-2019. *Nature*, 581(7809), 465–469.
- Pan, Y., Zhang, D., Yang, P., Poon, L. L., & Wang, Q. (2020). Viral load of SARS-CoV-2 in clinical samples. *The Lancet infectious diseases*, 20(4), 411–412.
- Van Doremalen, N., Bushmaker, T., Morris, D. H., et al. (2020). Aerosol and surface stability of SARS-CoV-2 as compared with SARS-CoV-1. *New England journal of medicine*, 382(16), 1564–1567.
- Pyankov, O. V., Bodnev, S. A., Pyankova, O. G., & Agranovski, I. E. (2018). Survival of aerosolized coronavirus in the ambient air. *Journal of aerosol science*, 115, 158–163.
- Ijaz, M. K., Brunner, A. H., Sattar, S. A., Nair, R. C., & Johnson-Lussenburg, C. M. (1985). Survival characteristics of airborne human coronavirus 229E. *Journal of General Virology*, 66(12), 2743–2748.
- Watanabe, T., Bartrand, T. A., Weir, M. H., Omura, T., & Haas, C. N. (2010). Development of a dose-response model for SARS coronavirus. *Risk Analysis: An International Journal*, 30(7), 1129–1138.
- Zhang, D., Liu, J., & Liu, L. (2020). On the capture of polar indoor air pollutants at sub-ppm level-A molecular simulation study. *Build. Simul.*, 13, 989–997.
- Das, P., Shrubsole, C., Jones, B., et al. (2014). Using probabilistic sampling-based sensitivity analyses for indoor air quality modelling. *Building and environment*, 78, 171–182.
- Wang, J., Huang, J., Feng, Z., et al. (2021). Occupant-density-detection based energy efficient ventilation system: Prevention of infection transmission. *Energy and Buildings*, 240, Article 110883.
- Feng, Z., Cao, S. J., & Haghighat, F. (2021). Removal of SARS-CoV-2 using UV+ Filter in built environment: simulation/evaluation by utilizing validated numerical method. *Sustainable Cities and Society*, Article 103226.
- Melikov, A. K., Ai, Z. T., & Markov, D. G. (2020). Intermittent occupancy combined with ventilation: An efficient strategy for the reduction of airborne transmission indoors. *Science of The Total Environment*, 744, Article 140908.
- Liao, M., Liu, H., Wang, X., et al. (2021). A technical review of face mask wearing in preventing respiratory COVID-19 transmission. *Current Opinion in Colloid & Interface Science*, Article 101417.
- Dada, A. C., & Gyawali, P. (2021). Quantitative microbial risk assessment (QMRA) of occupational exposure to SARS-CoV-2 in wastewater treatment plants. *Science of The Total Environment*, 763, Article 142989.
- Li, C., & Tang, H. (2021). Study on ventilation rates and assessment of infection risks of COVID-19 in an outpatient building. *Journal of Building Engineering*, Article 103090.
- Ribeiro, M. H. D. M., da Silva, R. G., Mariani, V. C., et al. (2020). Short-term forecasting COVID-19 cumulative confirmed cases: Perspectives for Brazil. *Chaos, Solitons & Fractals*, 135, Article 109853.
- da Silva, R. G., Ribeiro, M. H. D. M., Mariani, V. C., et al. (2020). Forecasting Brazilian and American COVID-19 cases based on artificial intelligence coupled with climatic exogenous variables. *Chaos, Solitons & Fractals*, 139, Article 110027.
- Mouratidis, K. (2021). COVID-19, internet, and mobility: The rise of telework, telehealth, e-learning, and e-shopping. *Sustainable Cities and Society*, Article 103182.
- Liu, Z., Liu, C., & Guan, C. (2021). The impacts of the built environment on the incidence rate of COVID-19: A case study of King County, Washington. *Sustainable cities and society*, Article 103144.
- Megahed, N. A., & Ghoneim, E. M. (2020). Antivirus-built environment: Lessons learned from Covid-19 pandemic. *Sustainable cities and society*, 61, Article 102350.
- Guo, Y., Qian, H., Sun, Z., et al. (2021). Assessing and controlling infection risk with Wells-Riley model and spatial flow impact factor (SPIF). *Sustainable Cities and Society*, 67, Article 102719.